PROCEEDINGS OF SCIENCE

$U(1)_A$ Breaking in Hot QCD in the Chiral Limit

Tamas G. Kovacs[a,b,*]

[a] *Institute of Physics and Astronomy, ELTE Eötvös Loránd University*
Pázmány Péter sétány 1/A, H-1117 Budapest, Hungary
[b] *Institute for Nuclear Research Bem tér 18/c, H-4026 Debrecen, Hungary*

E-mail: tamas.gyorgy.kovacs@ttk.elte.hu

We propose a simple instanton-based random matrix model of hot QCD that in the quenched case precisely reproduces the distribution of the lowest lattice overlap Dirac eigenvalues. Even after including dynamical quarks the model can be easily simulated in volumes and for quark masses that will be out of reach for direct lattice simulations in the foreseeable future. Our simulations show that quantities connected to the $U(1)_A$ and $SU(N_f)_A$ chiral symmetry are dominated by eigenvalues in a peak of the spectral density that becomes singular at zero in the thermodynamic limit. This spectral peak turns out to be produced by an ideal instanton gas. By generalizing Banks-Casher type integrals for the singular spectral density, definite predictions can be given for physical quantities that are essential to test chiral symmetry breaking, but presently impossible to compute reliably with direct lattice simulations.

The 41st International Symposium on Lattice Field Theory (LATTICE2024)
28 July - 3 August 2024
Liverpool, UK

*Speaker

PoS(LATTICE2024)012

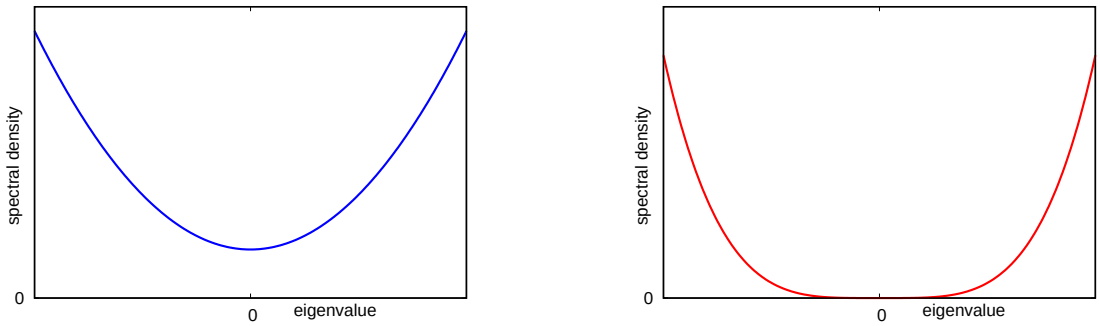

Figure 1: A schematic representation of the spectral density of the Dirac operator below the critical temperature in the hadronic phase (left), and above the critical temperature, in the quark-gluon plasma phase (right).

1. Introduction

Quantum chromodynamics (QCD), the theory of strong interactions has an approximate $SU(2)_L \times SU(2)_R \times U(1)_V \times U(1)_A$ symmetry. The flavor non-singlet vector symmetry is a result of the approximate equality of the masses of the two light quarks, the u and d, and the axial symmetries are there because both m_u and m_d are much lighter than the relevant QCD scale. Classically, the symmetries would all be exact if $m_u = m_d = 0$ were to hold exactly.

At low temperature the $SU(2)_L \times SU(2)_R$ symmetry is broken spontaneously, and it is only the diagonal vector subgroup of the symmetry that remains intact. However, at finite temperature, the transition to the quark-gluon plasma phase results in the restoration of the axial part of the symmetry $SU(2)_A$. The order parameter characterizing this transition is the chiral condensate $\langle\bar{\psi}\psi\rangle$. This can also be written in terms of the spectrum of the Dirac operator as

$$\langle\bar{\psi}\psi\rangle = \propto \frac{1}{V}\sum_k \frac{1}{i\lambda_k + m} \propto \int_{-\Lambda}^{\Lambda} d\lambda \frac{m}{\lambda^2 + m^2}\rho(\lambda) \xrightarrow[m\to 0]{} \rho(0), \tag{1}$$

where $i\lambda_k$ are the eigenvalues of the Dirac operator, and the sum over the eigenvalues can be written in terms of the Dirac spectral density $\rho(\lambda)$, using the symmetry $i\lambda \leftrightarrow -i\lambda$ of the spectrum. Due to the $\frac{m}{\lambda^2+m^2}$ factor, for small quark masses most of the contribution to the integral comes from the spectral region $|\lambda| \lesssim m$. As a result, in the chiral limit the only contribution is given by the spectral density at zero, which is the Banks-Casher formula [1]. In this way, the spectral density at zero can also serve as an oder parameter of the transition. In Fig. 1 we show a schematic plot of the spectral density in the low temperature, symmetry broken phase and in the high temperature phase where the symmetry is restored.

The spectrum of the Dirac operator can also be calculated in lattice simulations, and for a long time lattice results were in accordance with the above expectations; in the high temperature phase the spectral density appeared to vanish at zero virtuality. This was the situation until the appearance of chirally symmetric lattice Dirac operators, in particular the overlap [2]. The first hint at a more complicated picture appeared in Ref. [3], where a peculiar spike was found at high temperature in the spectrum at zero of the chirally symmetric overlap Dirac operator. This was a quenched

simulation on rather coarse lattices, and for a long time this spectral spike was largely ignored, most likely because it was considered a quenched or coarse lattice artifact.

Recently more detailed studies of the spectral spike appeared. In particular, evidence was found that it is neither a quenched nor a coarse lattice artifact, as the spike was found to be present on finer lattices both with and without dynamical quarks [4]. It was also suggested that the spectral spike was singular in the thermodynamic limit, and could signal a separate phase of QCD, intermediate between the finite temperature crossover and the even higher temperature perturbative regime [5]. The presence of the spike was also independently verified [6, 7], and shown also for sea quarks lighter than the physical u and d quarks [8]. More recently in a large scale study with staggered sea and valence quarks, the spectral peak was seen to be present in the continuum limit [9]. Quark eigenstates in the peak were found to exhibit nontrivial localization properties, hinting at the possible presence of another mobility edge, very close to zero in the spectrum [10–12], in addition to the already well established mobility edge higher up in the spectrum, separating localized modes from the bulk [13].

All the works cited in the above paragraph used staggered or other non-chiral sea quarks, although some utilized chiral (overlap) quarks for the valence. Since the spectral peak is a narrow structure close to zero, it is important for the Dirac operator to properly resolve the small Dirac eigenvalues, for which exact chiral symmetry is needed. This point is particularly important, since after integrating out the quarks, the partition function of QCD reads

$$Z = \int \mathcal{D}U \quad \prod_f \det\left(D[U] + m_{\mathrm{f}}\right) \cdot \mathrm{e}^{-S_{\mathrm{g}}[U]}, \tag{2}$$

where U is the gauge field configuration, $D[U]$ is the covariant Dirac operator and S_{g} is the gauge action. If the quark mass is small, the quark determinant is expected to suppress configurations with many small Dirac eigenvalues which might result in the disappearance of the spectral peak at zero. There are also studies using (close to) chiral quarks, namely domain wall quarks. Indeed, their conclusion is that for small but finite quark masses, the spectral peak is so suppressed that it cannot be detected at all [14–16]. For the most recent updates see [17, 18].

The spectral peak is not only important for the Banks-Casher relation, and the restoration of the flavor non-singlet chiral symmetry. As discussed in many of the above cited works (see also [19]), it also determines the fate of the $U(1)_A$ axial symmetry. It can be shown that if in the chiral limit the Dirac spectral density develops a gap at zero, or even if it is analytic at zero, the effects of the anomalous $U(1)_A$ symmetry breaking cannot be seen in scalar and pseudoscalar meson correlators [20]. The fate of the spectral spike is thus also essential for the $U(1)_A$ symmetry.

In the present paper I would like to ask and answer the following three questions. What is the physical origin of the spectral peak at zero that appears in high temperature QCD? How is it suppressed by the quark determinant if light dynamical quarks are present? How does the peak influence the fate of the flavor singlet and the flavor non-singlet axial symmetries in the chiral limit?

2. The spectral peak in quenched QCD

Since the quenched case is much simpler and there is general consensus about the presence of the spectral spike there, we start the discussion with the quenched theory. In Fig. 2 we show

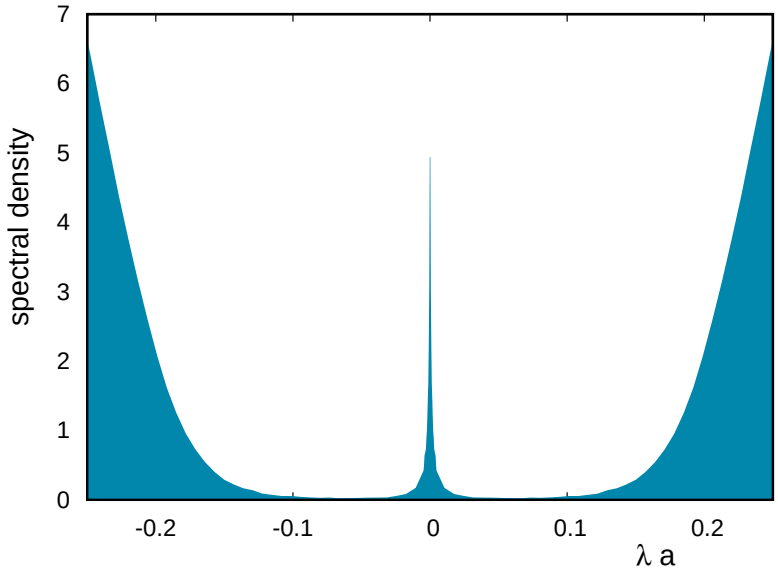

Figure 2: The spectral density of the overlap Dirac operator on a set of quenched gauge configurations with temporal size $N_t = 8$ and temperature $T = 1.05T_c$. The exact zero eigenvalues have been removed, they would show up as a delta function at zero.

a typical example of the overlap Dirac spectrum on quenched gauge field configurations slightly above the critical temperature. In the quenched case there is a genuine phase transition and thus T_c is well defined. The quenched simulation in question was done with the Wilson action at $\beta = 6.13$, corresponding to $T = 1.05T_c$ for the temporal lattice size $N_t = 8$. Since we are using the overlap Dirac operator, there are also exact zero eigenvalues in the spectrum, but those have been removed, they are not shown in the figure.

Starting from larger eigenvalues and going toward zero, the spectral density falls sharply, and it appears to go to zero, as expected in the symmetry restored phase. This behavior can also be qualitatively understood by noting that at finite temperature, due to the antiperiodic temporal boundary condition, the spectrum of free fermions have a gap around zero, equal to the lowest Matsubara frequency. If the fermions interact with the gauge field, the question is how the correlation length compares to the temporal box size, i.e. the inverse temperature. If the correlation length is smaller than $1/T$, then the fermions effectively "do not feel" the boundary condition, and there is no trace of the Matsubara gap; the spectrum extends with a nonzero density all the way down to the origin. In QCD this is exactly what happens in the chirally broken phase. On the other hand, if the correlation length is larger than $1/T$, even though there is no sharp Matsubara gap, the part of the spectrum below the lowest Matsubara frequency becomes heavily depleted.

This is exactly what we see in Fig. 2. However, at very small eigenvalues the spectral density starts to increase again, forming a sharp peak of near zero eigenvalues. In view of the foregoing discussion, this unnatural proliferation of small eigenvalues is certainly unexpected, and calls for an explanation. It was already suggested in Ref. [2] that the presence of instantons and anti-instantons might be responsible for the excess of small Dirac eigenvalues. Indeed, due to the Atiyah-Singer index theorem, if the gauge field configuration has topological charge Q, then the Dirac operator

has (at least) $|Q|$ exact zero eigenvalues with chirality plus or minus one, depending on the sign of Q [21]. In particular, each instanton and anti-instanton carries a zero mode of given chirality. In the presence of n_i instantons and n_a anti-instantons there are $|n_i - n_a|$ exact zero modes, while the rest of the would be zero modes will mix and split around zero. The splitting is governed by the distance between the topological objects and also their relative orientation in group space [22].

An important quantity characterizing the fluctuations of the topological charge is the topological susceptibility defined as

$$\chi = \frac{1}{V}\langle Q^2 \rangle, \tag{3}$$

where V is the four-volume of the system and the angled brackets denote expectation with respect to the path integral. Above the finite temperature transition the topological susceptibility falls sharply, and instantons form a dilute gas. The typical separation among instantons and anti-instantons is thus large, resulting in a small splitting of near zero modes around zero. This mechanism is a promising candidate to explain the spike in the spectral density.

At this point we have to make a remark about our use of the terminology. By *instanton* one typically means an exact solution of the Euclidean equation of motion, carrying and integer topological charge. There is ample evidence that in gauge configurations dominating the path integral, topological charge does not come in the form of pristine instantons (or calorons, the finite temperature exact solutions), not even well above the critical temperature. This can be seen from the fact that the dilute instanton gas approximation that assumes small fluctuations around the exact solution, cannot describe the dependence of the topological susceptibility on the temperature, seen in lattice simulations [23–25]. See also Ref.[26] for a recent update on the perturbative instanton calculation. In spite of all this, for simplicity we will use the word *instanton*, but by this we mean only well defined lumps of unit topological charge. We will show that the spike in the Dirac spectrum above T_c can be understood by assuming that the topological charge comes in the form of well separated lumps of unit charge.

3. Random matrix model of the zero mode zone of the Dirac operator

In what follows we would like to build a simple model of the subspace of the Dirac operator spanned by the would be zero modes that we call the zero mode zone (ZMZ). Our starting point is the simplest nontrivial configuration, that of an instanton and an anti-instanton at a distance r apart. In this case the ZMZ can be represented by the 2×2 matrix

$$D(A)_{\text{zmz}} = \begin{pmatrix} 0 & iw \\ iw & 0 \end{pmatrix}, \tag{4}$$

where

$$w \propto \mathrm{e}^{-\pi T r} \tag{5}$$

is the mixing between the instanton and anti-instanton zero mode. Since at high temperature the zero modes are exponentially localized with a localization length of $1/\pi T$ [27, 28], the mixing is also expected to be exponentially small in the distance r.

This can be easily generalized for the case when there are n_i instantons and n_a instantons present. Then the matrix of the Dirac operator in the ZMZ has the form

$$D(A)_{\text{zmz}} = \begin{array}{c} \overbrace{}^{n_i}\overbrace{}^{n_a} \\ \left(\begin{array}{c|c} 0 & iW \\ \hline iW^\dagger & 0 \end{array}\right) \end{array} \tag{6}$$

with two diagonal blocks of zeros and with the matrix elements

$$w_{ij} = A \times \exp(-\pi T \cdot r_{ij}), \tag{7}$$

r_{ij} denoting the distance of instanton i and anti-instanton j. The rank of this matrix is easily seen to be such that it has $|n_i - n_a|$ exact zero eigenvalues and the magnitude of the rest of the eigenvalues is controlled by the exponentially small off-diagonal matrix elements w_{ij}. The matrix also has exact chiral symmetry, as it anticommutes with γ_5 which in this basis takes a diagonal form with n_i -1-s and n_a $+1$-s in the diagonal. Given any instanton configuration, we can construct the matrix using the locations of the instantons and anti-instantons.

To complete the model we still have to decide how to choose the number of (anti-)instantons and their locations. It has been established that in quenched QCD, above T_c the distribution of the topological charge [29, 30], as well as that of the number of eigenvalues in the spike are consistent with a noninteracting, free instanton gas [31]. This suggests that we can choose the locations of the topological objects independently with a uniform spatial distribution. Since above T_c the typical instanton size is expected to be comparable to the temporal box size, we adopt a dimensionally reduced picture by choosing the instanton locations and measuring their distances in a 3D box of spatial size L^3, completely ignoring the temporal dimension. Finally, in a free instanton gas the distribution of the number of instantons and anti-instantons follows independent and identical Poisson distributions. The probability of having n_i instantons and n_a anti-instantons is thus

$$p(n_i, n_a) = \mathrm{e}^{-\chi V} \times \frac{(\chi V/2)^{n_i}}{n_i!} \times \frac{(\chi V/2)^{n_a}}{n_a!}, \tag{8}$$

where χ is the topological susceptibility, V is the four-volume. This completes the definition of our model. If the two parameters, the topological susceptibility and the prefactor A in Eq. (7) is known, we can produce an ensemble of random matrices that model the zero mode zone of the lattice Dirac operator.

To determine the two parameters, we computed the lowest part of the Dirac spectrum on an ensemble of $32^3 \times 8$ quenched lattice configurations at $T = 1.1T_c$. We determined the topological susceptibility by counting the number of exact zero eigenvalues, giving the topological charge on each configuration. The parameter A can be fitted to any feature of the lattice overlap Dirac spectrum. We chose to look at the distribution of the lowest nonzero eigenvalues, and could obtain a good fit of the whole distribution with the choice $A = 0.35$. This completes the fixing of the

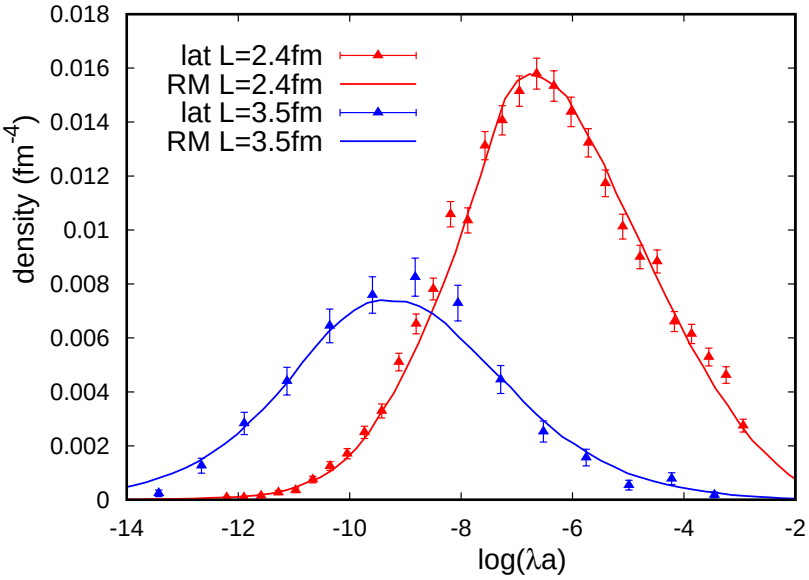

Figure 3: The distribution of the lowest overlap Dirac eigenvalue on two ensembles of quenched gauge configurations with different volumes. The temperature is $T = 1.1T_c$ in both cases, and for a better resolution of the small eigenvalues we plotted the distribution of the (natural) log of the eigenvalues. The triangles represent the lattice data, the continuous lines are calculated from the random matrix model. We used the smaller volume for fitting the parameter A, the larger volume is a prediction of the model without any further fitting.

parameters, and now we can test how well the resulting model describes the spectrum in different situations. A possible test is the distribution of the lowest eigenvalue on a larger volume. In Fig. 3 we compare the distribution of the lowest eigenvalue in the random matrix model to that of the lattice Dirac operator for two different volumes. The smaller volume with linear size $L = 2.5$ fm was used for fitting A, the larger volume, $L = 3.5$ fm is a prediction of the model that appears to agree with the lattice distribution. Several other tests can be performed for the distribution of higher eigenvalues in different volumes, also with restriction to a given topological charge sector, and in all cases the prediction of the model agrees with the lattice results. This indicates that the random matrix model, based on the free instanton picture gives an excellent description of the zero mode zone of the lattice overlap spectrum in the quenched case.

We would like to remark that the instanton-based random matrix model we propose here is not new. Already a long time ago it was extensively used in the context of instanton liquid models (see e.g. [22, 32]). What is new here is that our model is much simpler than the previous ones, as we use a dimensionally reduced 3D picture, ignore gauge interactions among topological lumps, and completely neglect the orientation of instantons in group space, as well as their nontrivial size distribution. These are all reasonable assumptions at high temperature in the quenched case. The other novelty of our model is that after fitting its two parameters, it can precisely describe the detailed features of the lattice overlap Dirac spectrum.

4. Full QCD, including dynamical quarks

So far we presented a simple random matrix model for describing the zero mode zone of the lattice overlap Dirac operator in the quenched case. Our goal in this section is to include dynamical quarks in the model. On the lattice this is done by including the fermion determinant $\det(D+m)^{N_\mathrm{f}}$ in the Boltzmann weight of each configuration. For simplicity, we will assume N_f degenerate quark flavors with mass m, but the generalization to different masses is straightforward. If the quark determinant is written in terms of the Dirac eigenvalues, it can be split into a product of two contributions, one coming from the eigenvalues in the zero mode zone, and the contribution of the rest of the spectrum that we call the bulk as

$$\det(D+m) = \prod_{\mathrm{zmz}}(\lambda_i+m) \times \prod_{\mathrm{bulk}}(\lambda_i+m). \tag{9}$$

The main observation here is that the bulk is separated from the ZMZ by a strongly depleted region in the spectrum, and the contribution of the bulk is not expected to be correlated with that of the ZMZ. Therefore, when computing expectations pertaining to the ZMZ, the bulk contribution gives only a constant factor, canceling in the expectations. In this way, when computing physical quantities dominated by the ZMZ, the contribution of the bulk to the determinant can be omitted. On the other hand, the contribution to the determinant of the ZMZ can be consistently computed within our random matrix model, and it can be added as an additional weight for each quenched instanton configuration. So the random matrix model of the ZMZ of full QCD will have the weight

$$P(n_i,n_a) \propto \underbrace{\mathrm{e}^{-\chi_0 V}\frac{1}{n_i!}\frac{1}{n_a!}\left(\frac{\chi_0 V}{2}\right)^{n_i+n_a}}_{\text{free instanton gas with random locations}} \times \det(D+m)^{N_\mathrm{f}} \tag{10}$$

for a given instanton configuration with n_i instantons and n_a anti-instantons. Here χ_0 is the quenched susceptibility, and the first part of the weight comes from the Poisson distributions of the free instanton gas, and the determinant of the random matrices is the extra reweighting factor due to the sea quarks. Although we have not indicated it explicitly, the determinant depends on the location of the topological objects.

5. Simulation of the random matrix model of the ZMZ of full QCD

In this section we present the results of a simulation of the random matrix model for two degenerate flavors of dynamical quarks. In Fig. 4 we show the topological susceptibility as a function of the quark mass. The triangles are the simulation data, and the continuous line is not a fit, but the quadratic function $\chi_0 m^2$, and it describes the simulation data perfectly.

To understand why this happens, let us first assume that the quark mass is much larger than the typical eigenvalues in the ZMZ. In this case the quark determinant can be approximated as

$$\prod_{n_i,n_a}(\lambda_i+m)^{N_f} \approx m^{N_f(n_i+n_a)}, \tag{11}$$

which means that in this approximation the determinant does not depend on the instanton locations, only on their numbers. This, in turn, implies that the reweighting with the determinant does not

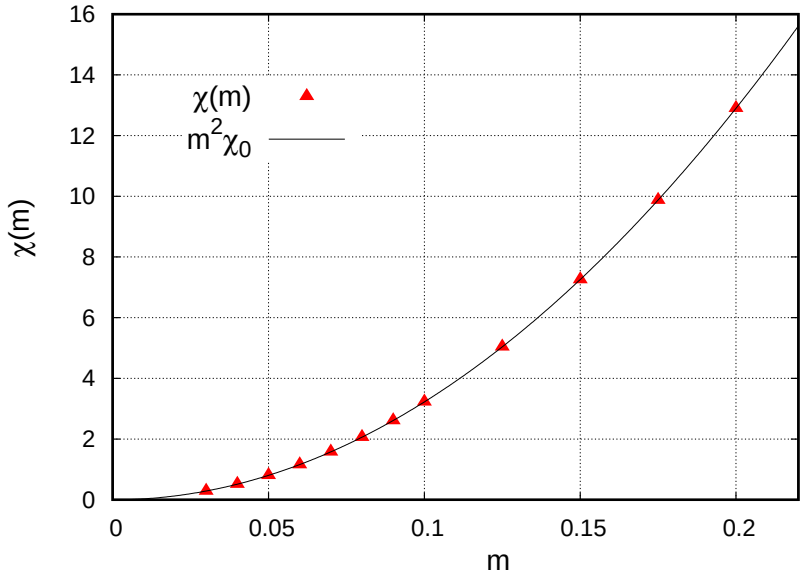

Figure 4: The topological susceptibility as a function of the quark mass, obtained from a simulation of the random matrix model, including the reweighting with the quark determinant for two degenerate quark flavors. The simulation data is plotted with triangles, and the continuous curve is not a fit, but the quadratic function $m^2\chi_0$, where χ_0 is the quenched topological susceptibility, the parameter of the model. Without the reweighting with the determinant, this would be the topological susceptibility.

introduce any interaction among the topological objects. Indeed, substituting the approximated determinant into Eq. (10), the $m^{N_f\,(n_i+n_a)}$ factor can be absorbed into the Poisson distributions as

$$P(n_i,n_a) \quad \propto \quad \left(\frac{\chi_0 V}{2}\right)^{n_i+n_a} \times \det(D+m)^{N_{\rm f}} \quad \approx \quad \left(\frac{m^{N_{\rm f}}\chi_0 V}{2}\right)^{n_i+n_a} \tag{12}$$

which, after proper normalization, results again in Poisson distributions for the number of instantons and anti-instantons, but with a density suppressed by the quark mass as $\chi_0 \to m^{N_{\rm f}}\chi_0$. In other words, if $|\lambda_i| \ll m$, then the matrix model with dynamical quarks still describes a free instanton gas, but with a smaller topological susceptibility.

What happens if the quark mass becomes smaller? To understand this, we write the determinant as

$$\det(D+m)^{N_{\rm f}} \quad = \quad m^{N_f\,(n_i+n_a)} \times \prod_i \left(1+\frac{|\lambda_i|^2}{m^2}\right), \tag{13}$$

where the last product is over the nonzero complex conjugate pairs of eigenvalues of the random matrix, representing the Dirac operator. If the quark mass is small, the power of the quark mass heavily suppresses those configurations that have many instantons. The configurations contributing to expectations have only a small number of instantons that are far apart. Since the matrix elements of the random matrix are exponentially small in the distance between the topological objects, the typical eigenvalues also become smaller and smaller as the instanton gas becomes more dilute. Consequently, no matter how small the quark mass is, the eigenvalues of the random matrices always remain much smaller than the quark mass, the last product of Eq. (13) is essentially equal

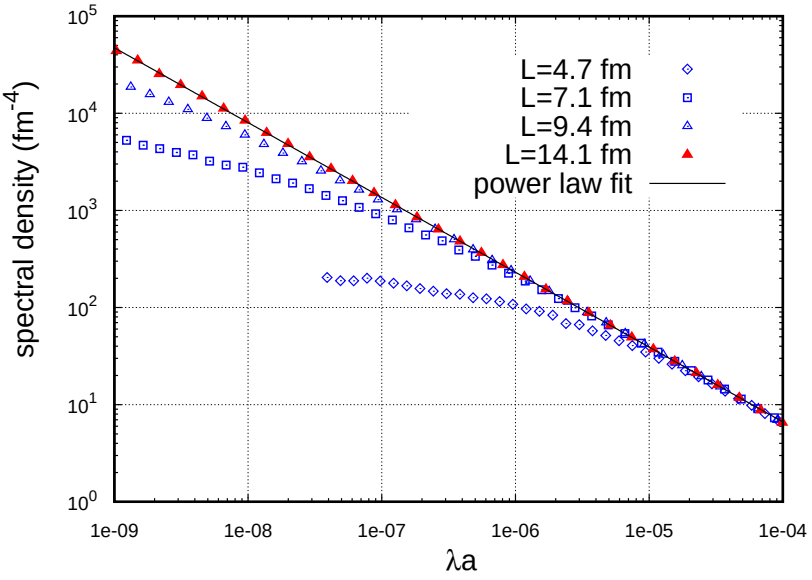

Figure 5: The spectral density of the quenched matrix model for different system sizes. The continuous line is a power-law fit to the common envelope of the curves, corresponding to different volumes.

to unity, and the approximation in Eq. (12) remains valid even in the chiral limit. This explains our finding that for two quark flavors the topological susceptibility is proportional to m^2, and the lowest part of the Dirac spectrum can be understood as the zero mode zone of a free instanton gas.

6. The nature of the spectral spike

Using the random matrix model, we can also study the spectral spike in more detail. As we already saw, independently of the quark mass, the lowest part of the spectrum can be attributed to a free instanton gas. Therefore, it is enough to simulate the quenched random matrix model. In the example we show, the parameters fitted to the quenched $T = 1.1T_c$ lattice data were used. In Fig. 5 we show the spectral density of the random matrix model. The exact zero eigenvalues have been removed from the spectrum, and we use log-log scale to be able to resolve the smallest eigenvalues. The different symbols correspond to simulations performed for systems of different sizes, indicated in the legends. The data points corresponding to different system sizes possess a common enveloping linear curve. This shows that in the infinite volume limit the spectral density is described by a singular power-law. In this particular case a linear fit to the envelope yields

$$\rho(\lambda) \propto \lambda^{\alpha} \quad \text{with} \quad \alpha = -0.770(5), \tag{14}$$

which is an integrable singularity.

Our experience shows that if the instanton gas becomes more dilute, the singularity gets stronger, i.e. α moves toward -1. We conjecture that in the chiral limit $\alpha \to -1$. At first sight this might seem counter-intuitive, as one would expect light dynamical quarks to repel the eigenvalues from zero. However, there is no contradiction, since even though in the chiral limit typical eigenvalues become smaller and the singularity gets stronger, the total number of eigenvalues in the singular

peak diminishes, and in the chiral limit vanishes, as expected. Singular behavior of the spectral density at zero in a similar instanton-based model was already found a long time ago by Sharan and Teper [33].

7. The fate of chiral symmetry in the chiral limit

According to the Banks-Casher formula, in the chiral limit the order parameter of chiral symmetry breaking is the spectral density at zero. We saw that in the high temperature phase the spectral density is singular at zero, and thus the Banks-Casher formula cannot be used. However, we can still go back to Eq. (1), the derivation of the Banks-Casher formula. Making use of the fact that even in the chiral limit the eigenvalues in the singular part of the spectral density are much smaller than the quark mass, we obtain

$$\langle\bar{\psi}\psi\rangle \propto \langle\sum_i \frac{m}{m^2+|\lambda_i|^2}\rangle \approx \underbrace{\left(\begin{smallmatrix}\text{avg. number of in-}\\ \text{stantons in free gas}\end{smallmatrix}\right)}_{m^{N_f}\chi_0 V} \times\frac{1}{m} = m^{N_f-1}\chi_0 V. \tag{15}$$

Here we used that if $|\lambda_i| \ll m$ then each term in the sum gives a contribution $1/m$, and after taking the expectation with the path integral, the average number of terms coincides with the average number of instantons (plus anti-instantons) in the free instanton gas, responsible for the singular spike. The upshot is that in the chiral limit the condensate is proportional to the $N_f - 1$-th power of the quark mass. As a result, for more than one flavor, the condensate vanishes in the chiral limit, as we expect from the restoration of the flavor non-singlet chiral symmetry. In the case of one flavor, the condensate does not vanish, but in this case there is no chiral symmetry to be broken or restored.

In recent years there have been a lot of discussion about how the anomalous $U(1)_A$ symmetry is manifested in the high temperature phase. A quantity that was extensively studied is the difference of the pion and delta susceptibility that is expected to be nonzero if the symmetry is broken. This can also be written as a Banks-Casher type spectral sum, for which the foregoing argument can again be used. Thus we obtain that in the chiral limit

$$\chi_\pi - \chi_\delta = \langle\sum_i \frac{m^2}{(m^2+\lambda_i^2)^2}\rangle \approx \underbrace{\left(\begin{smallmatrix}\text{avg. number of in-}\\ \text{stantons in free gas}\end{smallmatrix}\right)}_{m^{N_f}\chi_0 V} \cdot\frac{1}{m^2} = m^{N_f-2}\chi_0 V. \tag{16}$$

This behavior, and that in Eq. (15) is fully supported by direct simulations of our matrix model. Remarkably, for $N_f = 2$ the quantity $\chi_\pi - \chi_\delta$ is nonzero in the chiral limit. We emphasize that this happens in spite of the fact that in the chiral limit the topological susceptibility vanishes, but the anomaly still nontrivially affects the π minus δ susceptibility. This can happen only because the spectral density is singular at the origin. This scenario has another nontrivial consequence. Even though the spontaneously broken chiral symmetry is restored above T_c, the order of the thermodynamic and the chiral limit is still essential. If the chiral limit is taken first in a finite volume, then as can be seen in Fig. 5, the singularity at the origin is "regularized" by the finite volume, and $\chi_\pi - \chi_\delta$ becomes zero.

This argument also highlights the difficulties in seeing this effect in actual lattice simulations. The influence of the anomaly on these quantities, related to chiral symmetry is proportional to the

topological susceptibility. Even in the quenched case the topological susceptibility falls sharply above T_c, and light dynamical quarks suppress topological fluctuations even more. Therefore, at high temperatures the effect we described can be numerically small. If the volume is not large enough to contain typically several instantons and anti-instantons, the spectral spike does not form. In addition, to resolve the small eigenvalues in the spectral spike, one needs a chiral Dirac operator both for the sea, to account for the proper suppression of the small eigenvalues, and for the valence to have the correct contribution of the small eigenvalues to physical quantities.

8. Conclusions

We saw that the singular spike in the spectral density at the origin can be explained by mixing would be zero modes of a free gas of instantons and anti-instantons. This is consistent with constraints obtained for the spectral density from the assumption of the restoration of the spontaneously broken chiral symmetry [34, 35], and also consistent with the quasi-instanton picture of Kanazawa and Yamamoto [36, 37]. As we already remarked, instantons here do not mean field configurations close to solutions of the field equations, and they might not even mean well localized lumps of topological charge. Indeed, all that we can infer from the success of our model is that the would be zero modes are exponentially localized with exponentially small mixing matrix elements. Finding different localization properties in the gauge field and the zero modes would not be unnatural, as in contrast to the zero mode, the gauge field of the finite temperature caloron solution falls only like a power-law [38]. The topological charge density certainly has nontrivial structures [39], and exploring their relationship to the spatial structure of eigenmodes in the ZMZ would be interesting.

Our instanton-based random matrix model also predicts the appearance of some tightly bound instanton–anti-instanton pairs, in addition to the free instanton gas. However, in the chiral limit the splitting of the corresponding eigenvalues remains constant, governed by the small size of the molecules. Therefore, the corresponding eigenvalues do not appear in the singular spike, and they do not contribute to the quantities dominated by the spectral spike [40].

We showed that in one particular quantity, the pion minus delta susceptibility, for $N_f = 2$ light flavors the anomalous chiral symmetry breaking still shows up at high temperature in the chiral limit. Since our arguments are valid up to arbitrarily high but finite temperatures, the anomalous breaking of the $U(1)_A$ symmetry should remain up to arbitrarily high temperatures. However, the strength of the breaking was seen to be proportional to the topological susceptibility in the quenched limit at the given temperature. Since this susceptibility falls sharply with increasing temperature, the size of the symmetry breaking should also become very small, but still non-vanishing. This suggests that the $U(1)_A$ symmetry is not restored, but the manifestation of its breaking for different quantities is still an open question that has also a bearing on the nature of the transition in the chiral limit. This is a topic that has been recently extensively studied both in lattice simulations [41–44] and low energy effective models [45–49].

Acknowledgments

The author is supported by NKFIH grant K-147396 and excellence grant TKP2021-NKTA-64.

References

[1] T. Banks and A. Casher, *Chiral symmetry breaking in confining theories*, *Nucl. Phys. B* **169** (1980) 103.

[2] R. Narayanan and H. Neuberger, *A Construction of lattice chiral gauge theories*, *Nucl. Phys. B* **443** (1995) 305 [hep-th/9411108].

[3] R.G. Edwards, U.M. Heller, J.E. Kiskis and R. Narayanan, *Chiral condensate in the deconfined phase of quenched gauge theories*, *Phys. Rev. D* **61** (2000) 074504 [hep-lat/9910041].

[4] A. Alexandru and I. Horváth, *Phases of SU(3) Gauge Theories with Fundamental Quarks via Dirac Spectral Density*, *Phys. Rev. D* **92** (2015) 045038 [1502.07732].

[5] A. Alexandru and I. Horváth, *Possible New Phase of Thermal QCD*, *Phys. Rev. D* **100** (2019) 094507 [1906.08047].

[6] O. Kaczmarek, L. Mazur and S. Sharma, *Eigenvalue spectra of QCD and the fate of* $\mathrm{U}_A(1)$ *breaking towards the chiral limit*, *Phys. Rev. D* **104** (2021) 094518 [2102.06136].

[7] H.T. Ding, S.T. Li, S. Mukherjee, A. Tomiya, X.D. Wang and Y. Zhang, *Correlated Dirac Eigenvalues and Axial Anomaly in Chiral Symmetric QCD*, *Phys. Rev. Lett.* **126** (2021) 082001 [2010.14836].

[8] O. Kaczmarek, R. Shanker and S. Sharma, *Eigenvalues of the QCD Dirac matrix with improved staggered quarks in the continuum limit*, *Phys. Rev. D* **108** (2023) 094501 [2301.11610].

[9] A. Alexandru, C. Bonanno, M. D'Elia and I. Horváth, *Dirac spectral density in* $N_f = 2+1$ *QCD at* $T = 230$ MeV, *Phys. Rev. D* **110** (2024) 074515 [2404.12298].

[10] A. Alexandru and I. Horváth, *Unusual Features of QCD Low-Energy Modes in the Infrared Phase*, *Phys. Rev. Lett.* **127** (2021) 052303 [2103.05607].

[11] A. Alexandru and I. Horváth, *Anderson metal-to-critical transition in QCD*, *Phys. Lett. B* **833** (2022) 137370 [2110.04833].

[12] χQCD, CLQCD collaboration, *Separation of infrared and bulk in thermal QCD*, *J. High Energy Phys.* **12** (2024) 101 [2305.09459].

[13] M. Giordano and T.G. Kovács, *Localization of Dirac Fermions in Finite-Temperature Gauge Theory*, *Universe* **7** (2021) 194 [2104.14388].

[14] G. Cossu, S. Aoki, H. Fukaya, S. Hashimoto, T. Kaneko, H. Matsufuru et al., *Finite temperature study of the axial* U(1) *symmetry on the lattice with overlap fermion formulation*, *Phys. Rev. D* **87** (2013) 114514 [1304.6145].

[15] A. Tomiya, G. Cossu, S. Aoki, H. Fukaya, S. Hashimoto, T. Kaneko et al., *Evidence of effective axial U(1) symmetry restoration at high temperature QCD*, *Phys. Rev. D* **96** (2017) 034509 [1612.01908].

[16] JLQCD collaboration, *Study of the axial $U(1)$ anomaly at high temperature with lattice chiral fermions*, *Phys. Rev. D* **103** (2021) 074506 [2011.01499].

[17] JLQCD collaboration, *Axial U(1) symmetry near the pseudocritical temperature in $N_f = 2+1$ lattice QCD with chiral fermions*, *PoS* **LATTICE2023** (2024) 185 [2401.14022].

[18] D. Ward, S. Aoki, Y. Aoki, H. Fukaya, S. Hashimoto, I. Kanamori et al., *Study of symmetries in finite temperature $N_f = 2$ QCD with Möbius Domain Wall Fermions*, PoS **LATTICE2024** (2025) 346, [2412.06574].

[19] V. Azcoiti, *Spectral density of the Dirac-Ginsparg-Wilson operator, chiral U(1)A anomaly, and analyticity in the high temperature phase of QCD*, *Phys. Rev. D* **107** (2023) 114516 [2304.14725].

[20] S. Aoki, H. Fukaya and Y. Taniguchi, *Chiral symmetry restoration, eigenvalue density of Dirac operator and axial* U(1) *anomaly at finite temperature*, *Phys. Rev. D* **86** (2012) 114512 [1209.2061].

[21] M.F. Atiyah and I.M. Singer, *The Index of elliptic operators. 5.*, *Annals Math.* **93** (1971) 139.

[22] T. Schäfer and E.V. Shuryak, *Instantons in QCD*, *Rev. Mod. Phys.* **70** (1998) 323 [hep-ph/9610451].

[23] S. Borsányi et al., *Calculation of the axion mass based on high-temperature lattice quantum chromodynamics*, *Nature* **539** (2016) 69 [1606.07494].

[24] C. Bonati, M. D'Elia, M. Mariti, G. Martinelli, M. Mesiti, F. Negro et al., *Axion phenomenology and θ-dependence from $N_f = 2+1$ lattice QCD*, *J. High Energy Phys.* **03** (2016) 155 [1512.06746].

[25] P. Petreczky, H.-P. Schadler and S. Sharma, *The topological susceptibility in finite temperature QCD and axion cosmology*, *Phys. Lett. B* **762** (2016) 498 [1606.03145].

[26] A. Boccaletti and D. Nógrádi, *The semi-classical approximation at high temperature revisited*, *J. High Energy Phys.* **03** (2020) 045 [2001.03383].

[27] D.J. Gross, R.D. Pisarski and L.G. Yaffe, *QCD and Instantons at Finite Temperature*, *Rev. Mod. Phys.* **53** (1981) 43.

[28] M. García Pérez, A. González-Arroyo, C. Pena and P. van Baal, *Weyl-Dirac zero mode for calorons*, *Phys. Rev. D* **60** (1999) 031901 [hep-th/9905016].

[29] C. Bonati, M. D'Elia, H. Panagopoulos and E. Vicari, *Change of θ Dependence in 4D SU(N) Gauge Theories Across the Deconfinement Transition*, *Phys. Rev. Lett.* **110** (2013) 252003 [1301.7640].

[30] S. Borsanyi, Z. Fodor, D.A. Godzieba, R. Kara, P. Parotto, D. Sexty et al., *Topological features of the deconfinement transition*, *Phys. Rev. D* **107** (2023) 054514 [2212.08684].

[31] R.Á. Vig and T.G. Kovács, *Ideal topological gas in the high temperature phase of SU(3) gauge theory*, *Phys. Rev. D* **103** (2021) 114510 [2101.01498].

[32] E.V. Shuryak and J.J.M. Verbaarschot, *Random matrix theory and spectral sum rules for the Dirac operator in QCD*, *Nucl. Phys. A* **560** (1993) 306 [hep-th/9212088].

[33] UKQCD collaboration, *On the spectral density from instantons in quenched QCD*, *Phys. Rev. D* **60** (1999) 054501 [hep-lat/9812009].

[34] M. Giordano, *Constraints on the Dirac spectrum from chiral symmetry restoration*, *Phys. Rev. D* **110** (2024) L091504 [2404.03546].

[35] M. Giordano, *Constraints on the Dirac spectrum from chiral symmetry restoration and the fate of* $\mathrm{U}(1)_A$ *symmetry*, *PoS* **LATTICE2024** (2025) 188 [2412.02517].

[36] T. Kanazawa and N. Yamamoto, *Quasi-instantons in QCD with chiral symmetry restoration*, *Phys. Rev. D* **91** (2015) 105015 [1410.3614].

[37] T. Kanazawa and N. Yamamoto, U(1) *axial symmetry and Dirac spectra in QCD at high temperature*, *J. High Energy Phys.* **01** (2016) 141 [1508.02416].

[38] T.C. Kraan and P. van Baal, *Periodic instantons with nontrivial holonomy*, *Nucl. Phys. B* **533** (1998) 627 [hep-th/9805168].

[39] J.A. Mickley, W. Kamleh and D.B. Leinweber, *Numerical evidence for fractional topological objects in SU(3) gauge theory*, *Phys. Rev. D* **109** (2024) 094507 [2312.14340].

[40] T.G. Kovács, *Fate of Chiral Symmetries in the Quark-Gluon Plasma from an Instanton-Based Random Matrix Model of QCD*, *Phys. Rev. Lett.* **132** (2024) 131902 [2311.04208].

[41] O. Philipsen, *Lattice Constraints on the QCD Chiral Phase Transition at Finite Temperature and Baryon Density*, *Symmetry* **13** (2021) 2079 [2111.03590].

[42] F. Cuteri, O. Philipsen and A. Sciarra, *On the order of the QCD chiral phase transition for different numbers of quark flavours*, *J. High Energy Phys.* **11** (2021) 141 [2107.12739].

[43] S. Mitra, F. Karsch and S. Sharma, *Towards a parameter-free determination of critical exponents and chiral phase transition temperature in QCD*, *PoS* **LATTICE2024** (2025) 187 [2411.15988].

[44] G. Aarts et al., *Phase Transitions in Particle Physics: Results and Perspectives from Lattice Quantum Chromo-Dynamics*, *Prog. Part. Nucl. Phys.* **133** (2023) 104070 [2301.04382].

[45] G. Fejős, *Perturbative RG analysis of the condensate dependence of the axial anomaly in the three flavor linear sigma model*, *Symmetry* **13** (2021) 488 [2012.08706].

[46] G. Fejos, *Second-order chiral phase transition in three-flavor quantum chromodynamics?*, *Phys. Rev. D* **105** (2022) L071506 [2201.07909].

[47] G. Fejos and A. Patkos, *Thermal behavior of effective UA(1) anomaly couplings in reflection of higher topological sectors*, *Phys. Rev. D* **109** (2024) 036035 [2311.02186].

[48] G. Fejos and T. Hatsuda, *Order of the SU(Nf)×SU(Nf) chiral transition via the functional renormalization group*, *Phys. Rev. D* **110** (2024) 016021 [2404.00554].

[49] F.L. Braghin, $U_A(1)$ *symmetry-breaking quark interactions from vacuum polarization*, *Eur. Phys. J. A* **60** (2024) 178 [2405.00880].